

Article

Improved PVTOL Test Bench for the Study of Over-Actuated Tilt-Rotor Propulsion Systems

Luis Amezcua-Brooks ^{1,†} , Eber Maciel-Martínez ^{1,†} and Diana Hernandez-Alcantara ^{2,*} 

¹ Facultad de Ingeniería Mecánica y Eléctrica, Universidad Autónoma de Nuevo León, San Nicolás de los Garza 66455, NL, Mexico; luis.amezquitabr@uanl.edu.mx (L.A.-B.); eber.macielm@uanl.edu.mx (E.M.-M.)

² School of Engineering and Technologies, Universidad de Monterrey, San Pedro Garza García 66238, NL, Mexico

* Correspondence: diana.hernandez@udem.edu

† These authors contributed equally to this work.

Abstract: In recent years, applications exploiting the advantages of tilt-rotors and other vectored thrust propulsion systems have become widespread, particularly in many novel Vertical Takeoff and Landing (VTOL) configurations. These propulsion systems can provide additional control authority, enabling more complex flight modes, but the resulting control systems can be challenging to design due to the mismatch between the vehicle degrees of freedom and physical input variables. These propulsion systems present both advantages and difficulties because they can exert the same overall forces and moments in many different propulsive configurations. This leads to the traditional non-uniqueness problem when using the inverse dynamics control allocation approach, which is the basis of many popular VTOL control algorithms. In this article, a modified Planar VTOL (PVTOL) test bench configuration, which considers an arbitrary number of co-linear tilting rotors, is introduced as a benchmark for the study of the control allocation problem. The resulting propulsion system is then modeled and linearized in a closed and compact form. This allows a simple and systematic derivation of many of the currently used control allocation approaches. According to the proposed PVTOL configuration, a two-rotor test bench is implemented experimentally and a decoupling control allocation strategy based on Singular Value Decomposition (SVD) analysis is developed. The proposed approach is compared with a traditional input mixer algorithm based on physical intuition. The results show that the SVD-based solution achieves better cross-coupling reduction and preserves the main properties of the physically derived approach. Finally, it is shown that the proposed PVTOL configuration is effective for studying the control allocation problem experimentally in a controlled environment and could serve as a benchmark for comparing different approaches.

Keywords: PVTOL; test bench; VTOL; control allocation; cross-coupling



Citation: Amezcua-Brooks, L.; Maciel-Martínez, E.; Hernandez-Alcantara, D. Improved PVTOL Test Bench for the Study of Over-Actuated Tilt-Rotor Propulsion Systems. *Machines* **2024**, *12*, 46. <https://doi.org/10.3390/machines12010046>

Academic Editor: Tao Li

Received: 21 November 2023

Revised: 18 December 2023

Accepted: 18 December 2023

Published: 10 January 2024



Copyright: © 2024 by the authors. Licensee MDPI, Basel, Switzerland. This article is an open access article distributed under the terms and conditions of the Creative Commons Attribution (CC BY) license (<https://creativecommons.org/licenses/by/4.0/>).

1. Introduction

Recently, *Vertical Takeoff and Landing* (VTOL) aircraft configurations have attracted a high degree of interest from the research community and the aeronautics industry. The novelty of these vehicles introduces a set of challenging issues because many of the well-established design methodologies, used for conventional aircraft configurations, do not apply directly. This has also attracted the attention of the authorities, which have proposed several novel specifications to address many of these challenges (see, for example, [1,2]).

The majority of the reports found in the literature deal with a specific VTOL configuration. For instance, in [3,4], the authors study a commonly used arrangement, in which the tilt-rotors are used to generate either lift force in hover or thrust force in horizontal flight (i.e., as the one used in the V-22 Osprey). In this case, the authors propose a nonlinear observer and control approach to stabilize the vehicle with good results. Many other aspects of this configuration have been researched, for instance, in [5], the dynamic properties of

the vehicle are studied by calculating the linear stability and control derivatives of the vehicle. This study shows that it is possible to evaluate the well-known flight modes of a traditional airplane such as phugoid, short period, Dutch roll, and spiral subsidence. Using a similar approach. In [6], it is shown that a linear control approach can be used to stabilize the full nonlinear dynamics of the vehicle. In this case, the authors noticed a serious degree of cross-coupling when the vehicle operated in helicopter mode. A similar configuration, which considers that the aircraft remains in hover with a vertical fuselage orientation, is studied in [7]. In this report, the authors used a scheduled linear control approach to stabilize the vehicle. These reports show that, although this VTOL configuration results in a highly coupled and nonlinear system, the use of linear control approaches is preferred in some instances due to its simplicity and the possibility of evaluating the closed loop dynamics in terms of classical flight dynamics modes.

Although the configuration mentioned in the previous paragraph is common, it is far from being the only one used in VTOL applications. In particular, tilt-rotors can be found in several configurations, ranging from all the rotors being tilt-rotors to a single rotor used as a tilt-rotor. For instance, in [8], a fixed-wing aircraft with one fixed and two tilting rotors is presented. In this case, a set of nested control loops with linear controllers is used to stabilize the vehicle. Several reviews dealing with VTOL configurations can be found in the literature [9–11]. From these reports, the following insights can be obtained:

- There is a high degree of heterogeneity in the propulsion system configurations, including number, distribution, and operating conditions.
- There is an increasing use of distributed tilting rotors (or similar thrust vectoring elements).
- The multiplicity of propulsors and control surfaces results in a high number of control inputs, introducing an over-actuation problem, which is normally denoted as the *control allocation problem* in the literature (although under-actuation problems have also been treated as allocation problems by some authors).
- The control allocation problem is commonly dealt with by separating the vehicle into two parts: (1) a rigid body, which is driven by virtual control inputs (i.e., force and moment vectors), and (2) the propulsion subsystem, which is driven in such a way that the desired force and moment vectors are obtained. In practice, it is difficult to pair specific physical inputs to a particular force or moment component without introducing cross-coupling in the rigid body control loop.
- Although many control approaches have been proposed, linear *Proportional Integral Derivative (PID)* controllers are still used in many practical setups due to their simplicity and low computational overhead.

The control allocation problem is one of the main issues found in novel vehicle configurations with many tilting propulsors. The simplest approach for the allocation problem consists of pairing specific physical inputs with the desired outputs in a fully decentralized control manner. In other cases, physical insight allows proposing a simple allocation strategy [8]. Although these approaches have been used for traditional configurations (i.e., classical pairings, such as elevator surface and pitch angle), many novel VTOL configurations cannot be operated using this scheme due to excessive cross-coupling.

In cases where the cross-coupling introduced by a simple control allocation algorithm is excessive, a preferred approach consists of establishing virtual (decoupled) inputs and attempting to solve the inverse actuator dynamics to determine the necessary physical inputs [9]. This approach is easy and effective if the propulsion subsystem inverse dynamics exist and are unique. A well-known example of this is the typical quad-rotor control allocation algorithm, where a vector of four virtual inputs is related to the angular velocities of the four propellers through a fixed and invertible 4x4 matrix [12]. It is also interesting to note that this approach has proven to be highly successful even though the propulsion model used to derive it is arguably over-simplified, as it neglects several important aerodynamic factors [13]. This proves that it is possible to obtain effective allocation solutions using simplified propulsion models.

In more recent years, VTOL configurations have become more complex so that inverse propulsion dynamics either do not exist or are not unique. In particular, over-actuated systems are more common due to the increased number of actuators. In these cases, a simple solution consists of using physical insights to add additional constraints to reduce the dimension of the control input vector. For example, in [14], the control allocation for a spacecraft using two kinds of actuators was solved by a proportional distribution of the desired control torque considering the characteristics of each actuator. Physical insight has also been used to refine *Cascade-Generalized Inversion (CGI)* approaches, such as in [15], where a test bench for a vehicle with multiple tilting rotors was controlled by grouping several physical actuators in a hierarchical manner. There are also several mathematical tools which can aid in solving the allocation problem, such as the Moore–Penrose pseudo-inverse matrix and the *Karush–Kuhn–Tucker (KKT)* optimality conditions [16]. Many of these approaches rely on a linear approximation approach, whose range can be expanded by the use of scheduling techniques [16]. Non-linear approaches have been also proposed; however, the resulting solutions can be too taxing for the computational systems on board small vehicles. Therefore, fast linear or scheduling approaches are still preferred in many applications [16,17].

More recently, in [17], a review article dealing with the taxonomy of vehicles with multiple rotors showed that there are still many challenges in the study of these propulsion systems. Among these, the heterogeneity of the propulsion configurations, the aerodynamic interaction of the various actuators (also noted in [13]), and the actuator limitations (including actuator saturation and response times) are the most relevant. One of the tools observed in [17] which has been used to overcome some of these problems is the use of co-linear or co-planar propulsor arrangements.

The previous paragraphs illustrate how the popularization of VTOL vehicles with a wide range of configurations, particularly those that contain an arbitrary number of tilting rotors, has motivated the study of the control allocation problem, from both theoretical and practical points of view. In this context, it is appropriate to recall that during the emergence of the modern quad-copter drone, in the early 2000s and later, several novel technical and theoretical developments were made. One of the tools that proved to be very valuable for researchers was the so called *Planar Vertical Takeoff and Landing (PVTOL)* configuration, which was widely adopted by researchers in a simplified two *degrees of freedom (DoF)* test bench version. This simplified model allowed both researchers and prospective control engineers to study novel control strategies and to perform preliminary experimental tests in a safe environment before performing actual flight tests. The sheer number of contributions to control, sensor, and modelling theory that still rely on the PVTOL configuration is a testament to its usefulness. From neural network backstepping control [18] to the study of robust feedback linearization [19] and noise-rejecting active disturbance controllers [20], the PVTOL model is still widely used by researchers. In many ways, the PVTOL has become a de facto benchmark platform.

While the PVTOL is a good approximation of simple vehicles such as the quad-copter, this simplification fails to capture the main difficulties of many current VTOL vehicles. In particular, many of these vehicles include some form of tilt-rotor or other similar thrust vectoring propulsion system. There have been some attempts to propose a more general PVTOL configuration, which also include the complications of tilting rotors. For example, in [21], a tilting rotor PVTOL was introduced with good results; however, in this report, only simulations are presented and the allocation problem is reduced by neglecting the reactive torque of the propellers.

Finally, a summary of the main elements found in the literature review is as follows:

- There is a high level of heterogeneity in the propulsion configuration of recent VTOL vehicles with a movement towards a higher number of actuators.
- The resulting control allocation problems are highly dependent on the propulsion configuration. Therefore, the study of this issue can yield vehicle-specific results.

- The use of simplified test benches (such as the PVTOL) can aid in the study of prospective control strategies while preserving many of the dynamic and experimental complexities, allowing a more rapid development of novel/better solutions.
- The typical PVTOL test bench configuration is unable to represent many of the difficulties found in recent VTOL vehicles.
- Although non-linear control and allocation approaches can deliver improved performance for wider operating ranges, in many *Unmanned Aerial Vehicle (UAV)* applications, linear controllers and allocation approaches are still being used and researched due to their simplicity and efficiency.

Considering the previous context, in this article, the control allocation problem is studied both theoretically and experimentally. In particular, the following elements are presented:

- A novel PVTOL test bench configuration containing an arbitrary number of co-linear tilting rotors is proposed as a progression of the traditional PVTOL test bench configuration. This configuration can reproduce several of the interesting issues found in novel VTOL vehicles, mainly the control allocation and cross-coupling problems. In addition, this configuration can be easily extended to include an arbitrary number of co-planar tilting propulsors, so that a wider range of vehicles can be mimicked.
- A general method for obtaining a closed form of the linearization of the propulsion model for the modified PVTOL configuration is presented. This can be useful because, as mentioned before, many control allocation strategies depend on it.
- A simple test bench, based on the modified PVTOL configuration, is implemented experimentally. This simple test bench allows testing control allocation and cross-coupling problems.
- A simple decoupling control allocation scheme for the test bench, based on a linear approximation derived through *Singular Value Decomposition (SVD)*, is presented. This approach allows defining an optimal solution for the allocation problem of the modified PVTOL configuration. The resulting optimization can solve the over-actuation problem by introducing a wide range of considerations. In this case, low-error and practical physical considerations are used.
- The proposed SVD control allocation approach is compared with a more traditional input mixer algorithm, derived from physical insight, both through simulations and using the experimental test bench. The results show that the proposed control allocation scheme allows decreasing the cross-coupling with a simple static decoupling matrix.

The authors also want to emphasize that the test bench presented here (as well as the proposed allocation algorithm) should be considered an initial step towards a generalized study of the control allocation problem through the use of a prospective standardized test bench configuration based on the modified PVTOL configuration. The authors believe that the proposed test bench could be used by the scientific community for this purpose; however, those seeking additional complexity may consider adding more co-linear propulsors (or even co-planar propulsors in an arbitrary matrix configuration). This would result in an even more complex over-actuation problem. The authors hope that the use of such a family of test benches could potentially become a widely used benchmark as an aid in the study and development of novel propulsion systems for VTOL vehicles.

2. Materials and Methods

2.1. A PVTOL with an Arbitrary Number of Co-Linear Tilting Rotors

This section introduces a PVTOL test bench with an arbitrary number of co-linear tilting rotors and derives the linearization of the resulting propulsion system model in a compact and closed form. This propulsion configuration was chosen because it can replicate many of the control allocation problems found in a wide range of vehicles and can be easily extended to a more complex arbitrary co-planar propulsion system by simple aggregation. In comparison with the typical PVTOL experimental test bench configuration,

which is restricted to a single DoF (pitch angle), the proposed configuration adds yaw angle as an additional DoF. This enables the introduction of a multivariable control problem (i.e., two outputs instead of one), which facilitates a better study of the control allocation problem.

It must be noted that adding further DoFs to the test bench (for example, roll angle) could increase its research potential at the cost of increased mechanical complexity. In this regard, it is important to recognize that a successful test bench benchmark must balance the trade-off between its mechanical/manufacturing complexity and its research value potential. To support this claim, consider the classical PVTOL test bench, which is normally restricted to pitch angle movement. Although this restriction is clearly not completely representative of vehicles such as the quad-copter, as mentioned in the introduction, this has not precluded the classical PVTOL test bench from being used for a wide range of studies related to quad-rotor applications. In this case, the proposed configuration remains simple enough to be cost- and mechanically accessible, but complex enough for the control allocation and multivariable cross-coupling problems to appear. Therefore, we believe that the proposed configuration (in particular, the two-rotor version presented in an upcoming section) represents a similar sweet spot for these problems, as the classical PVTOL test bench is for the typical quad-rotor.

Figure 1 shows the propulsion system with an arbitrary number (n) of tilting rotors, where the distance of each rotor from the center of gravity is denoted by l_i and the tilt angle of each rotor is denoted by δ_i , with $i = 1, 2, 3, \dots, n$. The figure also depicts the angular positions and rates of the PVTOL in a typical inertial North-East-Down (NED) reference frame, where θ and ψ denote the pitch and yaw angles, respectively, and q and r denote the pitch and yaw rates, respectively.

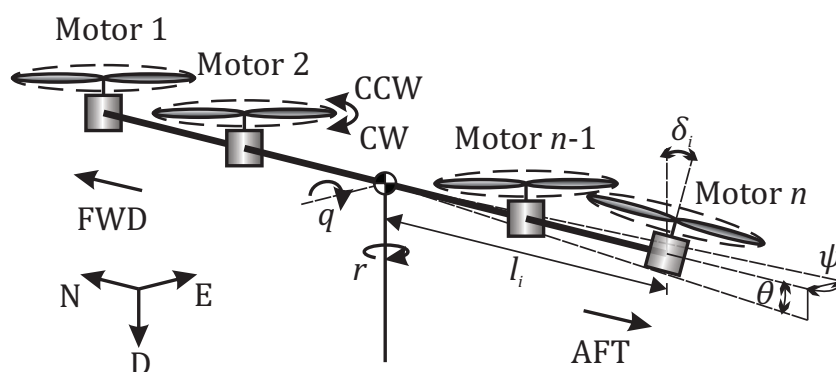


Figure 1. Modified PVTOL configuration with n tilting propulsors.

Each motor/propeller induces a thrust force T_i and a moment R_i aligned with its tilt angle, as shown in Figure 2. Because R_i is produced by rotational drag, its direction is opposite to the propeller rotation. According to simplified propeller modelling, typically used for multi-rotor vehicles, force T_i and moment R_i can be modelled as [13]:

$$\begin{aligned} T_i &= \frac{1}{2}\rho S C_T \omega_i^2 \\ R_i &= \frac{1}{2}\rho S C_Q \omega_i^2 \end{aligned} \tag{1}$$

where S is the disc area of the propeller, C_T is the thrust coefficient, C_Q is the reactive moment coefficient, ρ is the air density, and ω_i is the angular speed of propeller i . Accordingly, R_i can be rewritten as $R_i = k_i T_i$ with $k_i = C_Q/C_T$, which is convenient to reduce the number of independent input variables.

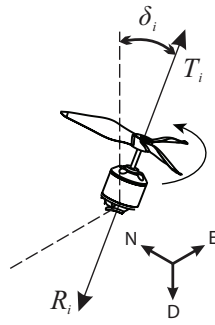


Figure 2. Thrust force (T_i) and reactive moment (R_i) produced by a single propeller.

This article studies the control allocation problem for the pitching and yawing moments, denoted as M and N , respectively, since these are the two natural degrees of freedom for a test bench with the modified PVTOL configuration of Figure 1. Following this configuration, the resulting pitching and yawing moments are:

$$\begin{aligned} M &= \sum_{i=1}^n T_i l_i \cos \delta_i (-1)^{\alpha_i} - \sum_{i=1}^n T_i k_i \sin \delta_i (-1)^{\beta_i} \\ N &= \sum_{i=1}^n T_i k_i \cos \delta_i (-1)^{\beta_i} + \sum_{i=1}^n T_i l_i \sin \delta_i (-1)^{\alpha_i} \end{aligned} \quad (2)$$

with:

$$\alpha_i = \begin{cases} 0, & \text{if position FWD} \\ 1, & \text{if position aft} \end{cases} \quad (3)$$

$$\beta_i = \begin{cases} 0, & \text{if rotation CCW} \\ 1, & \text{if rotation CW} \end{cases} \quad (4)$$

where CW, CCW, and FWD denote *clockwise*, *counterclockwise*, and *forward* respectively.

For instance, considering a simple two-rotor arrangement, with a FWD propeller ($i = 1$) rotating CCW and an aft propeller ($i = 2$) rotating CW, the resulting moment equations yield:

$$\begin{aligned} M &= T_1 l_1 \cos \delta_1 - T_2 l_2 \cos \delta_2 - T_1 k_1 \sin \delta_1 + T_2 k_2 \sin \delta_2 \\ N &= T_1 k_1 \cos \delta_1 - T_2 k_2 \cos \delta_2 + T_1 l_1 \sin \delta_1 - T_2 l_2 \sin \delta_2 \end{aligned} \quad (5)$$

Although the non-linear propulsion model given by Equations (2) and (5), is useful for many applications, such as simulation, evaluation, and non-linear control design, many control allocation methods are based on a linear representation of the propulsion subsystem. As follows, the linear approximation of the two-propeller case will be derived and then extended for the general case.

The linear approximation of (5) is given by the Jacobian matrix P of the moment vector $[M \ N]^T$, that is:

$$\begin{bmatrix} \Delta M \\ \Delta N \end{bmatrix} = P \begin{bmatrix} \Delta T_1 \\ \Delta \delta_1 \\ \Delta T_2 \\ \Delta \delta_2 \end{bmatrix} \quad (6)$$

with

$$P = \begin{bmatrix} \frac{\partial M}{\partial T_1} & \frac{\partial M}{\partial \delta_1} & \frac{\partial M}{\partial T_2} & \frac{\partial M}{\partial \delta_2} \\ \frac{\partial N}{\partial T_1} & \frac{\partial N}{\partial \delta_1} & \frac{\partial N}{\partial T_2} & \frac{\partial N}{\partial \delta_2} \end{bmatrix}_0 \quad (7)$$

where $[\Delta M \ \Delta N]^T$ and $[\Delta T_1 \ \Delta \delta_1 \ \Delta T_2 \ \Delta \delta_2]^T$ are the resulting linear output and input vectors, and the sub-index 0 denotes evaluation in the equilibrium point.

Matrix P is also called the *propulsion matrix* in the literature and its properties (e.g., range) are a determining factor when calculating the physical control inputs (i.e., $[T_1 \ \delta_1 \ T_2 \ \delta_2]^T$)

necessary to reach a desired combination of input moments (i.e., $[MN]^T$). In this case, since the control inputs vector $\in \mathbb{R}^4$, while the moment vector $\in \mathbb{R}^2$, this PVTOL configuration yields an over-actuation problem, which will be studied in more detail later in the article.

From (6), it follows that:

$$P = \begin{bmatrix} l_1 \cos \delta_1 - k_1 \sin \delta_1 & -T_1 l_1 \sin \delta_1 - k_1 T_1 \cos \delta_1 & -l_2 \cos \delta_2 + k_2 \sin \delta_2 & T_2 l_2 \sin \delta_2 + k_2 T_2 \cos \delta_2 \\ l_1 \sin \delta_1 + k_1 \cos \delta_1 & T_1 l_1 \cos \delta_1 - k_1 T_1 \sin \delta_1 & -l_2 \sin \delta_2 - k_2 \cos \delta_2 & -T_2 l_2 \cos \delta_2 + k_2 T_2 \sin \delta_2 \end{bmatrix}_0 \quad (8)$$

Matrix P can be further decomposed as:

$$P = AP_1 = \begin{bmatrix} l_1 & -k_1 & -l_2 & k_2 \\ k_1 & l_1 & -k_2 & -l_2 \end{bmatrix} \begin{bmatrix} \cos \delta_1 & -T_1 \sin \delta_1 & 0 & 0 \\ \sin \delta_1 & T_1 \cos \delta_1 & 0 & 0 \\ 0 & 0 & \cos \delta_2 & -T_2 \sin \delta_2 \\ 0 & 0 & \sin \delta_2 & T_2 \cos \delta_2 \end{bmatrix}_0 \quad (9)$$

Furthermore, matrix P_1 can also be decomposed as:

$$P_1 = BC = \begin{bmatrix} \cos \delta_1 & -\sin \delta_1 & 0 & 0 \\ \sin \delta_1 & \cos \delta_1 & 0 & 0 \\ 0 & 0 & \cos \delta_2 & -\sin \delta_2 \\ 0 & 0 & \sin \delta_2 & \cos \delta_2 \end{bmatrix}_0 \begin{bmatrix} 1 & 0 & 0 & 0 \\ 0 & T_1 & 0 & 0 \\ 0 & 0 & 1 & 0 \\ 0 & 0 & 0 & T_2 \end{bmatrix}_0 \quad (10)$$

Therefore, matrix P can be rewritten as:

$$P = ABC = \begin{bmatrix} l_1 & -k_1 & -l_2 & k_2 \\ k_1 & l_1 & -k_2 & -l_2 \end{bmatrix} \begin{bmatrix} \cos \delta_1 & -\sin \delta_1 & 0 & 0 \\ \sin \delta_1 & \cos \delta_1 & 0 & 0 \\ 0 & 0 & \cos \delta_2 & -\sin \delta_2 \\ 0 & 0 & \sin \delta_2 & \cos \delta_2 \end{bmatrix}_0 \begin{bmatrix} 1 & 0 & 0 & 0 \\ 0 & T_1 & 0 & 0 \\ 0 & 0 & 1 & 0 \\ 0 & 0 & 0 & T_2 \end{bmatrix}_0 \quad (11)$$

Following the structure of (11), a generalization for the system with n propulsors can be derived. In particular, following a similar analysis, the linearization of the full non-linear propulsion subsystem (2) is given by:

$$\begin{bmatrix} \Delta M \\ \Delta N \end{bmatrix} = P \begin{bmatrix} \Delta T_1 \\ \Delta \delta_1 \\ \vdots \\ \Delta T_n \\ \Delta \delta_n \end{bmatrix} \quad (12)$$

where $P = ABC$ and $A \in \mathbb{R}^{2 \times 2n}$, $B \in \mathbb{R}^{2n \times 2n}$, and $C \in \mathbb{R}^{2n \times 2n}$.

As follows, each of the elements which comprise (12) will be derived in a closed and compact form. First, matrix A , which contains information regarding the location and orientation of each rotor, can be written as the concatenation of sub-matrices A_i :

$$A = [A_1 \quad A_2 \quad \cdots \quad A_n] \quad (13)$$

with

$$A_i = \begin{bmatrix} l_i (-1)_i^\alpha & k_i (-1)^{\beta_i+1} \\ k_i (-1)_i^\beta & l_i (-1)_i^\alpha \end{bmatrix} \quad (14)$$

In addition, B comprises a set of 2D rotation sub-matrices as:

$$B = \text{diag}\{B_1, B_2, \dots, B_n\} \quad (15)$$

with

$$B_i = \begin{bmatrix} \cos \delta_i & -\sin \delta_i \\ \sin \delta_i & \cos \delta_i \end{bmatrix}_0 \quad (16)$$

Finally, matrix C contains information regarding the equilibrium thrust of each propeller:

$$C = \text{diag}\{C_1, C_2, \dots, C_n\} \quad (17)$$

with

$$C_i = \begin{bmatrix} 1 & 0 \\ 0 & T_i \end{bmatrix}_0 \quad (18)$$

This completes the derivation of the linear approximation of the propulsion subsystem of the PVTOL of Figure 1. The structure obtained here is useful because it allows separating the three main physical properties that determine the resulting propulsion matrix P . In particular:

- Matrix A contains information regarding the physical position and rotation direction of each propeller. Since these properties are normally constant, updating matrix A is not necessary when calculating a linear approximation on a different operating point. However, analyzing its structure could be useful to determine which particular propulsive configuration is better for particular applications.
- Matrix B contains information regarding the tilt angle of each of the propellers. Depending on the operating range and behavior of the propulsion system, this matrix could be the most sensible for operating point modifications, and should be updated accordingly in scheduling approaches.
- Matrix C contains information regarding the thrust force of each propeller. This matrix could also require regular updates in a scheduling approach depending on the operating behavior of the vehicle.

In many cases, matrices B and C may not require a full update if only a sub-set of rotors change their operating point. Instead, updating sub-matrices B_i and C_i may be sufficient.

Although, in this case, the derivation and decomposition of the propulsion matrix was performed for the modified PVTOL, it may be possible that a similar decomposition could be useful for other complex propulsion systems, which is the motivation for this analysis (i.e., as a proof of concept).

2.2. Experimental Test Bench

In this section, an experimental test bench considering the modified PVTOL configuration proposed in the previous section is introduced. The schematic of the test bench is shown in Figure 3a, while Figure 3b shows the actual prototype. Although this is a simple two-rotor setup, this configuration yields an over-actuated system (as noted in the previous section); thus, it is sufficient to study the control allocation problem.

The test bench consists of a base with a transverse rod connecting a servo-motor at each end. Two bearings allow the system to move freely on two degrees of freedom. Brushless motors with propellers are attached to each of the servo-motors. A summary of the technical specifications of the test bench is as follows:

- Two 2304 Racestar brushless motors (81 W max power).
- Two Gemfan 51466 three-blade propellers, one CW and one CCW.
- Two MG995 servo-motors.
- One BNO055 absolute orientation sensor.

The orientation angles are measured using the BNO055 absolute orientation sensor array, which consists of a 3-axis accelerometer and gyroscope combined with a Kalman filter for the pitch and yaw angle reconstruction. These kinds of sensors are normally able to deliver measurements with a mean error of under 1.5 deg/s and 0.5 m/s² for the gyroscope and accelerometer, respectively [22–24]. This configuration can yield a low level

of angle measurement error in applications where no axial acceleration is present, so that the main source of measured acceleration is the gravity, as in the present application [25].

The test bench was operated with an external power source with a fixed voltage of 12 V, which provided enough current for all the operating conditions tested. The control algorithms were implemented in an ATmega2560 microcontroller, which is a low-power 8-bit micro controller capable of 6 MIPS at 16 MHz. The possibility to implement the proposed control allocation algorithm in this low-computational-power microcontroller is a salient characteristic, since most low-cost autopilot UAV solutions have limited computational power.

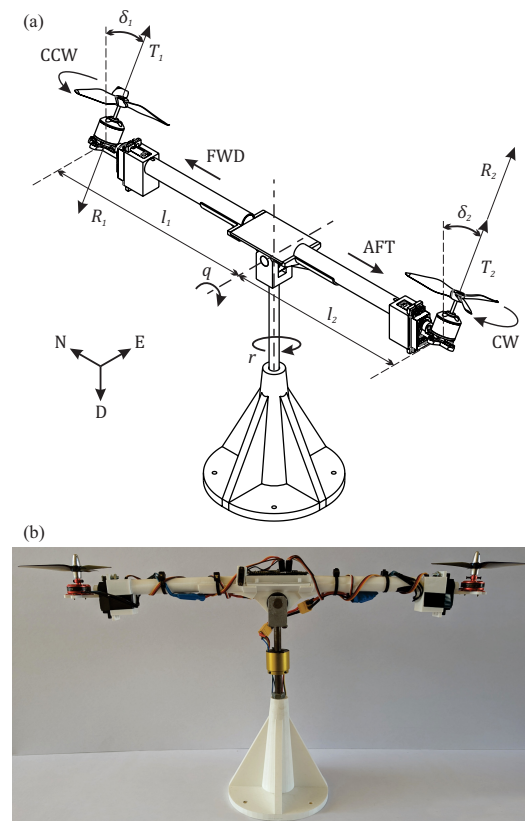


Figure 3. (a) Test bench schematic. (b) Physical prototype.

The microcontroller code was directly generated with Simulink/Matlab without further optimization operating at a sampling rate of 5 ms. Figure 4 shows the overall Simulink program used for the implementation of the control algorithms presented in this article.

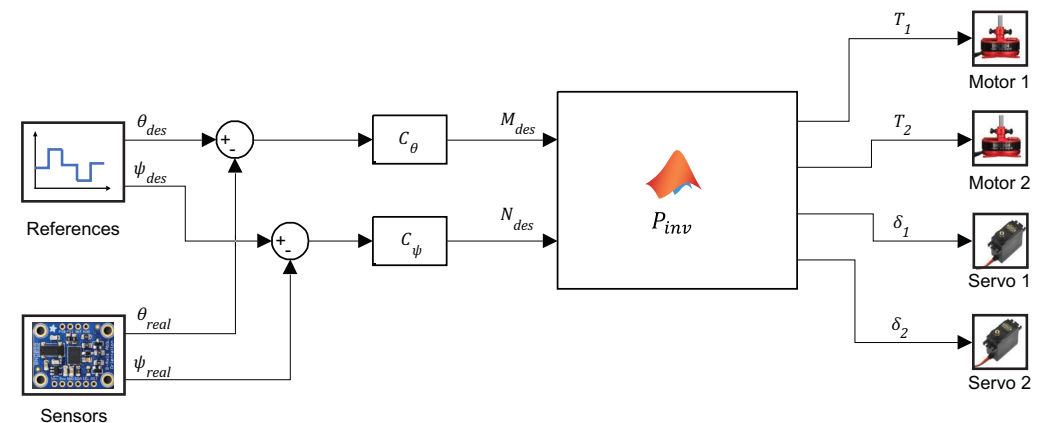


Figure 4. Simulink program for test bench.

An Atmel-based microcontroller board was programmed for the test bench. A summary of the resulting input and output variables for the test bench is shown next.

- Input variables:
 - Right motor thrust T_1 ;
 - Left motor thrust T_2 ;
 - Tilt angle of right motor δ_1 ;
 - Tilt angle of left motor δ_2 .
- Output variables:
 - Pitch rate $\dot{\theta} = q$;
 - Yaw rate $\dot{\psi} = r$;
 - Pitch angle θ ;
 - Yaw angle ψ .

Further details regarding the experimental and simulation setups are shown in Section 3, together with the corresponding experiments and simulations.

Recalling Equation (5), the resulting motion equations are given by:

$$\begin{aligned} I_{yy}\dot{q} &= T_1 l_1 \cos \delta_1 - T_2 l_2 \cos \delta_2 - T_1 k_1 \sin \delta_1 + T_2 k_2 \sin \delta_2 \\ I_{zz}\dot{r} &= T_1 k_1 \cos \delta_1 - T_2 k_2 \cos \delta_2 + T_1 l_1 \sin \delta_1 - T_2 l_2 \sin \delta_2 \end{aligned} \quad (19)$$

where I_{yy} and I_{zz} are the pitch and yaw inertial masses, respectively.

Accordingly, the resulting model considering the linearized propulsion model yields:

$$\begin{bmatrix} I_{yy} & 0 \\ 0 & I_{zz} \end{bmatrix} \begin{bmatrix} \Delta \dot{q} \\ \Delta \dot{r} \end{bmatrix} = P \begin{bmatrix} \Delta T_1 \\ \Delta \delta_1 \\ \Delta T_2 \\ \Delta \delta_2 \end{bmatrix} \quad (20)$$

with $P \in \mathbb{R}^{2 \times 4}$ as in Equation (11).

2.3. Control Allocation Problem

The objective is to design a linear controller for the pitch and yaw angles of the test bench using the input vector $[T_1 \delta_1 T_2 \delta_2]^T$. According to (20), this results in an over-actuated and a multivariable control problem. Although there are several control approaches which can deal with multivariable cross-coupling, an ideal approach would be to have an input-decoupling scheme which incorporates two virtual inputs, that is:

$$\begin{bmatrix} I_{yy} & 0 \\ 0 & I_{zz} \end{bmatrix} \begin{bmatrix} \Delta \dot{q} \\ \Delta \dot{r} \end{bmatrix} = \begin{bmatrix} M_{des} \\ N_{des} \end{bmatrix} \quad (21)$$

where M_{des} and N_{des} are the two arbitrary virtual inputs.

Therefore, in this case, the control allocation problem consists in finding a matrix P_{inv} such that $I = PP_{inv}$ so that the required physical input variables can be calculated for a particular value of the desired virtual inputs, that is:

$$\begin{bmatrix} T_1 \\ \delta_1 \\ T_2 \\ \delta_2 \end{bmatrix} = P_{inv} \begin{bmatrix} M_{des} \\ N_{des} \end{bmatrix} \quad (22)$$

In this article, two approaches to solve the control allocation problem will be compared: (1) a decentralized control approach based on physical intuition and (2) a mathematical approach based on SVD and optimization.

2.3.1. Physical Intuition-Based Decentralized Control Allocation

In this section, a proposal for the input signal mixer will be derived based on physical intuition and the following assumptions:

- A decentralized control approach for the pitch and yaw angles is sufficient to stabilize the test bench. This implies that pitch and yaw moments are derived separately without considering their interaction. This normally implies, for instance, that when calculating the pitch angle input mixer (directly related to M_{des}), it is assumed that $N_{des} = 0$. In addition, if the pitch angle mixer also affects the yawing moment N , then these effects are neglected, or at best considered as input perturbations for the yaw angle controller. That is, any residual cross-coupling is neglected.
- A small range of operation for the tilt-rotors is enough to stabilize the test bench. This assumption allows maintaining the focus of this study on the linear elements of the control allocation problem, which is the basis of most scheduling approaches. Later, it will be confirmed experimentally that indeed only small tilt angles are required for the stabilization of this PVTOL configuration. Nonetheless, extension of these results for wider operating ranges will be forthcoming in future studies.

For small angles, the system tends to behave as a classical PVTOL configuration with a single degree of freedom in the pitch angle and propeller thrust as inputs. In this case, the resulting pitching moment yields:

$$M = l_1 T_1 - l_2 T_2 \quad (23)$$

Thus, it is reasonable to use the differential thrust of propellers to induce pitching moment. In addition, when no pitching moment is required, it is also desirable for both propellers to maintain a specific equilibrium thrust T_0 . This yields the well-known PVTOL pitching moment input mixer:

$$T_1 = T_0 + \frac{M_{des}}{2l_1} \quad T_2 = T_0 - \frac{M_{des}}{2l_2} \quad (24)$$

On the other hand, in the case of the yaw angle, if $T_1 \approx T_2$ (i.e., $M_{des} \approx 0$), then the yawing moment yields:

$$N = T_1(k_1 \cos \delta_1 - k_2 \cos \delta_2) + T_1(l_1 \sin \delta_1 - l_2 \sin \delta_2) \quad (25)$$

Accordingly, noticing that $T_1 \approx T_2$ in (24) implies $T_1 \approx T_0$, the small angle approximation for the yawing moments is:

$$N = T_0 l_1 \delta_1 - T_0 l_2 \delta_2 \quad (26)$$

Therefore, the input mixer for the yawing moment is proposed as:

$$\delta_1 = \frac{N_{des}}{2T_0 l_1} \quad \delta_2 = -\frac{N_{des}}{2T_0 l_2} \quad (27)$$

Equations (24) and (27) will be used for the decentralized control allocation approach. It is clear that in this case, the pitching moment is achieved by modifying the propeller thrust, whereas the yawing moment is achieved by modifying the rotor tilt angle. Therefore, this solution is also easy to understand and to implement.

2.3.2. Singular Value Decomposition Control Allocation

In this section, a simple control allocation solution will be derived using the SVD analysis of the linearization of the propulsion system. Recalling Equation (6), the SVD of matrix P yields:

$$P_{2 \times 2n} = U_{2 \times 2} S_{2 \times 2n} V_{2n \times 2n}^T \quad (28)$$

where the sub-indexes show the size of each matrix.

Matrix S is a rectangular diagonal matrix called the *singular values matrix*, whose diagonal elements s_i are always positive, typically written in descending order, and are called the *singular values* of matrix P . In addition, matrices S and V are orthogonal. The rank of matrix P is equal to the number of non-zero singular values. Thus, matrix P can be

considered as a linear transformation of R^{2n} into R^{r_s} , where $r_s = \text{rank}(S)$ is the number of non-zero s_i values, which in this case, since $S \in R^{2 \times 2n}$, can only be at most 2. Finally, this analysis shows that for the modified PVTOL configuration with arbitrary number of tilting rotors, a fully decoupling control allocation solution exists **iff** $r_s = 2$.

The SVD of matrix P also allows viewing the linear transformation between an input vector $u \in R^{2n}$ and an output vector $y \in R^2$ as a series of intermediate linear transformations, as shown in Figure 5, where the intermediate transformed vectors are $y_2 \in R^{2n}$ and $y_1 \in R^2$, that is:

$$y_2 = V^T u \quad y_1 = S y_2 \quad y = U y_1 \tag{29}$$

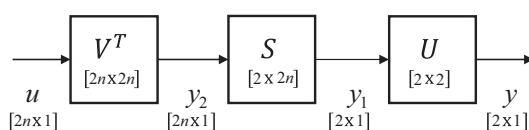


Figure 5. Decomposition of the linear transformation matrix P into intermediate transformations.

Figure 5 shows that the loss of dimension introduced by matrix P occurs in the intermediate transformation $y_1 = S y_2$ and is due to the rank of matrix S . In particular, matrix S has the following structure:

$$S = \begin{bmatrix} S_1 & 0_{2 \times 2n-2} \end{bmatrix} \tag{30}$$

where $0_{2 \times n-2}$ denotes a zero matrix of the indicated size and S_1 is given by:

$$S_1 = \text{diag}\{s_1, s_2\} \tag{31}$$

If the rank of P is two (i.e., S_1 is invertible), then all the possible input combinations u which produce a particular desired output y can be calculated with:

$$\begin{aligned} y_1 &= U^T y \\ y_{2S} &= S_1^{-1} y_1 \\ y_2 &= \begin{bmatrix} y_{2S} \\ y_{2N} \end{bmatrix} \\ u &= V y_2 \end{aligned} \tag{32}$$

where $y_{2N} \in R^{2n-2}$ is an arbitrary vector which does not have any effect over the resulting output vector y .

If $y_{2N} = 0$, then Equation (32) yields the Moore–Penrose pseudo-inverse. In particular, y_{2N} introduces additional degrees of freedom which account for the null subspace of S . The process of using this pseudo-inverse transformation to calculate an input u which produces a particular desired output y is represented in Figure 6. This allows injecting an arbitrary vector y_{2N} which can be selected according to additional practical considerations. Note that in this case, the SVD analysis was preferred over the direct pseudo-inverse approach because of the additional flexibility that the SVD decomposition yields, such as more precise control of the null space injection and information contained in matrices S and V .

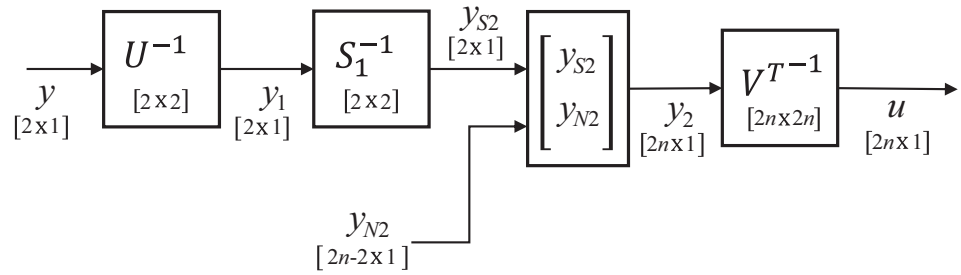


Figure 6. Graphical representation of using the pseudo-inverse to calculate input u from the desired output y .

2.3.3. SVD-Based Control Allocation Configuration

In the previous section, a control allocation approach based on SVD was presented for the general case of n co-linear tilting rotors. This method introduced additional degrees of freedom which could be potentially used to better comply with additional specifications. In this section, the SVD control allocation method will be applied to the two-rotor modified PVTOL test bench and the additional degrees of freedom will be configured according to practical considerations.

Considering the physical parameters of the test bench, and the equilibrium points reported in Table 1, the propulsion matrix P (i.e., the linear approximation of the propulsion system) yields:

$$P = \begin{bmatrix} 0.2050 & -0.0424 & -0.2050 & 0.0424 \\ 0.0103 & 0.8446 & -0.0103 & -0.8446 \end{bmatrix} \tag{33}$$

Table 1. Test bench parameters and equilibrium points.

Variable	Value
T_{1_0}	4.12 N
T_{2_0}	4.12 N
δ_{1_0}	0°
δ_{2_0}	0°
$l_{1,2}$	0.205 m
$k_{1,2}$	0.0103 m

Using Equations (28) and (32) with $u = [T_1 \ \delta_1 \ T_2 \ \delta_2]^T$ and $y = [M_{des} \ N_{des}]^T$ yields:

$$\begin{bmatrix} T_1 \\ \delta_1 \\ T_2 \\ \delta_2 \end{bmatrix} = \begin{bmatrix} 2.433 & 0.122 & 0.707 & -0.025 \\ -0.029 & 0.592 & 0.025 & 0.707 \\ -2.433 & -0.122 & 0.707 & -0.025 \\ 0.029 & -0.592 & 0.025 & 0.707 \end{bmatrix} \begin{bmatrix} M_{des} \\ N_{des} \\ a \\ b \end{bmatrix} \tag{34}$$

where the vector containing the additional degrees of freedom is given by $y_{2N} = [a \ b]^T$.

Parameters a and b can be selected freely according to the designer considerations. In this case, the first consideration is that it is desirable that $\delta_1 = \delta_2 = 0$ when $M_{des} = N_{des} = 0$. Physically, this implies that, in equilibrium, the rotors should point upwards. Therefore, from (34), it is required that

$$0.025a + 0.707b = 0 \tag{35}$$

Thus, b is set as:

$$b = -0.035a \tag{36}$$

Next, parameter a is selected so that the quadratic error considering the non-linear propulsion model is minimized. This yields the following minimization problem:

$$\min_a J = (e_M^2 + e_N^2) \tag{37}$$

with:

$$\begin{bmatrix} e_M \\ e_N \end{bmatrix} = \begin{bmatrix} M \\ N \end{bmatrix} - P P_{inv}(a) \begin{bmatrix} M_{des} \\ N_{des} \end{bmatrix} \quad (38)$$

where M and N are as in Equation (5), P is from (33), and $P_{inv}(a)$ is matrix (34) with an arbitrary a value.

A simple numerical exercise, shown graphically in Figure 7, reveals that the optimal value for this parameter is $a = 5.82$.

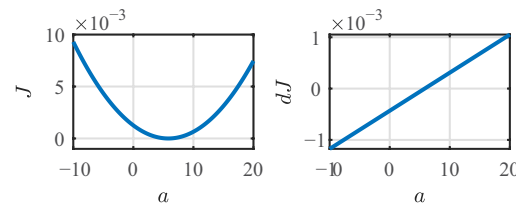


Figure 7. Cost function J and its derivative (dJ) as a function of a .

Finally, the resulting input mixer yields:

$$\begin{bmatrix} T_1 \\ \delta_1 \\ T_2 \\ \delta_2 \end{bmatrix} = \begin{bmatrix} 2.433M_{des} + 0.122N_{des} + 4.12 \\ -0.029M_{des} + 0.592N_{des} \\ -2.433M_{des} - 0.122N_{des} + 4.12 \\ 0.029M_{des} - 0.592N_{des} \end{bmatrix} \quad (39)$$

2.3.4. Final Mixer Algorithm Comparison

In this section, the resulting mixer algorithms using both approaches will be compared for T_1 and δ_1 (note that T_2 and δ_2 are similar). In particular, the decentralized control approach using the parameters of Table 1 and Equations (24) and (27) yields:

$$T_{1,dec} = 4.12 + 2.43M_{des} \quad \delta_{,dec} = 0.592N_{des} \quad (40)$$

On the other hand, from Equation (39), using the SVD approach yields:

$$T_{1,dec} = 4.12 + 2.43M_{des} + 0.122N_{des} \quad \delta_{,dec} = 0.592N_{des} - 0.029M_{des} \quad (41)$$

Examination of Equations (40) and (41) reveals that both approaches arrive at similar results, with the main difference being that the SVD approach introduces additional decoupling factors. In addition, this also shows that the selection of the free parameters during the SVD approach design is an important element which allowed for the incorporation of similar physical insights as the decentralized approach.

3. Results

3.1. Simulation Results

In this section, the effectiveness of both control allocation approaches is tested through simulations using the control scheme shown in Figure 8, where the inverse propulsion system dynamics (i.e., P_{inv}) is obtained according to the control allocation schemes of the previous section.

A pair of PID controllers was designed for the pitch and yaw angles, C_θ and C_ψ , respectively, using Equation (21) as a design model. That is, it was assumed that the propulsion system is fully decoupled and compensated. This assumption yields a pair of simple double-integrator dynamics, which are controlled through direct pole placement and the specifications of Table 2. These specifications aim at introducing a certain degree of bandwidth separation between the orientation angles and consider a slower response time for the propeller tilting servos than the propeller thrust. This aspect will become an important issue for the experimental implementation and is commented on later in the article. The resulting PID gains are reported in Table 3.

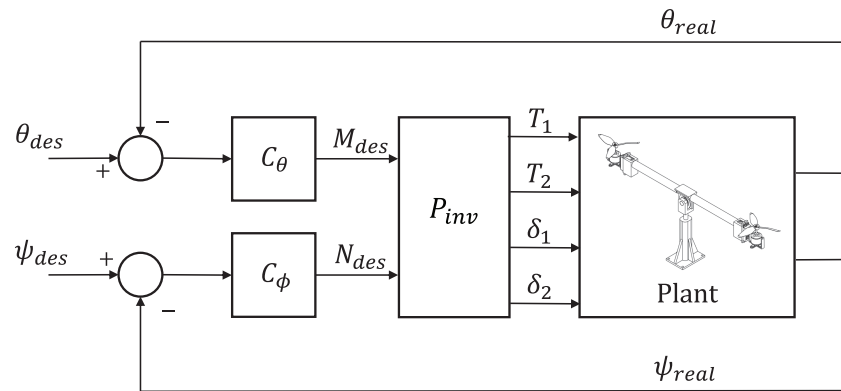


Figure 8. Test bench control system scheme. In this case, P_{inv} represents the control allocation algorithm.

Table 2. Specifications.

Requirement	Pitch θ	Yaw ψ
Overshoot M_p	<35%	<25%
Settling Time T_s	<11 s	<15 s

Table 3. Simulation PID controller gains.

Constant	Pitch	Yaw
Proportional	2	1.5
Integral	0.1	0.1
Derivative	1.5	1

The simulations were performed with both control allocation approaches (i.e., *decentralized* and *SVD-decoupled*), the previously mentioned PID controllers and the non-linear model of the modified PVTOL test bench from Equation (19). In order to assess the resulting cross-coupling due to the input mixer algorithms, the following conditions were simulated:

1. Pitch-Varying Case: The pitch θ reference changes in steps, while the yaw ψ reference remains constant at zero.
2. Yaw-Varying Case: The yaw ψ reference changes in steps, while the pitch θ reference remains constant at zero.

3.1.1. Pitch-Varying Case

Figure 9a shows the simulated responses of the pitch and yaw angles for the decentralized approach, while Figure 9b presents the same variables using the SVD-decoupling algorithm. This figure shows that while the pitch angle response of both approaches is similar and within the control specifications, the cross-coupling introduced in the yaw angle is significantly greater in the case of the decentralized input mixer.

In order to better assess the effectiveness of the SVD-decoupling control allocation approach, Figure 10 presents a comparison between the reference moments (i.e., M , N and M_{des} , N_{des}) and the actual moments exerted by the propulsion system for the simulation of Figure 9 with the SVD-decoupling approach. This figure shows that the resulting SVD-decoupling mixer has a very low error level (N and M deltas) and very good tracking capabilities. The greatest error level is observable in the case of the yawing moment at the time of the pitch angle step movement, which is when the propulsion system cross-coupling is at its highest.

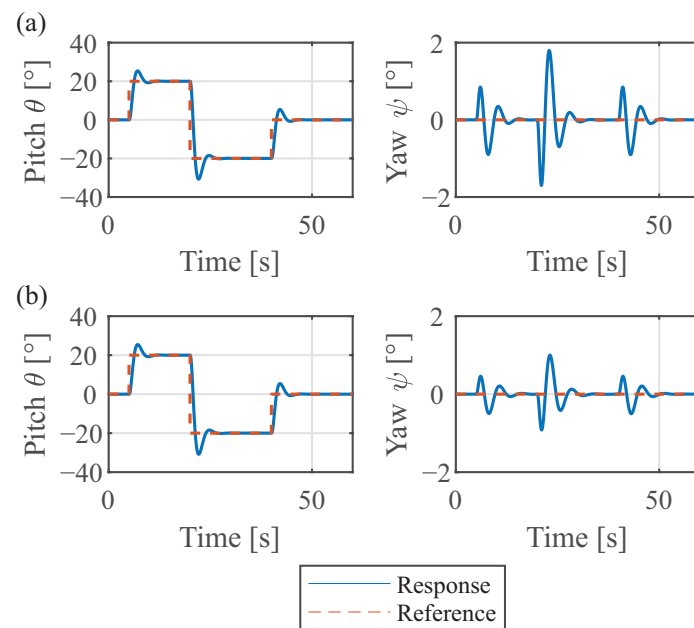


Figure 9. Pitch θ varying simulated responses. (a) Decentralized control allocation approach. (b) SVD-decoupling control allocation approach.

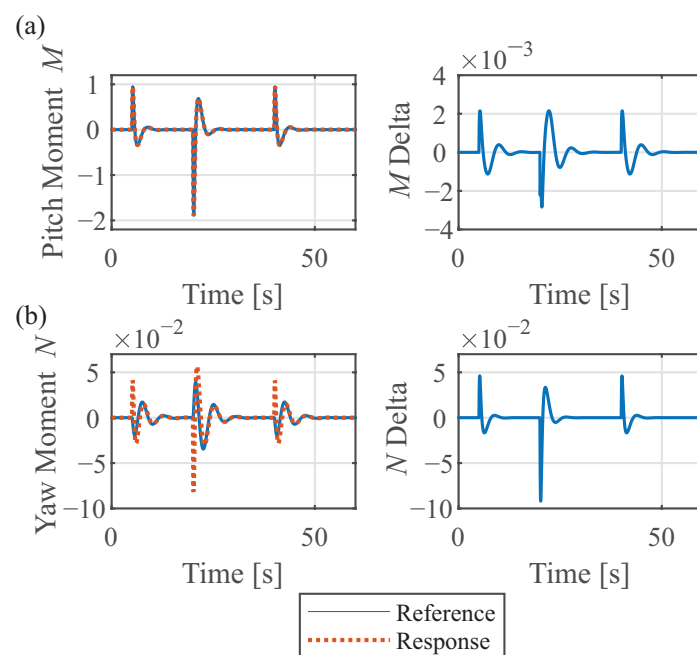


Figure 10. Comparison between reference moments and the actual moments exerted by the propulsion system for the SVD-decoupling control allocation approach (a) Pitching moment M . (b) Yawing moment N .

3.1.2. Yaw-Varying Case

For the yaw variation simulations, Figure 11a shows the simulated responses of the pitch and yaw angles for the decentralized approach, while Figure 11b presents the same variables using the SVD-decoupling algorithm. Similarly to the pitch-varying case, the cross-coupling in the pitch angle due to variations in the yaw angle reference is reduced by using the SVD-decoupling mixer.

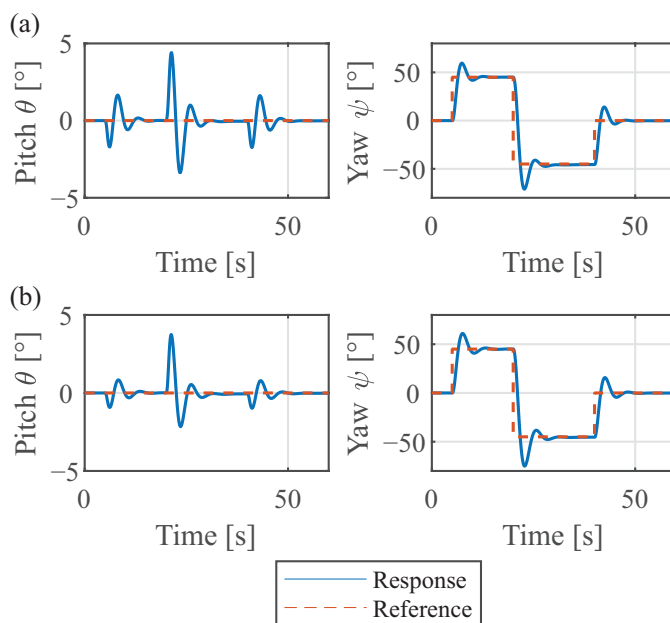


Figure 11. Yaw ψ varying simulated responses. (a) Decentralized control allocation approach. (b) SVD-decoupling control allocation approach.

Finally, Figure 12 presents a comparison between the reference moments (i.e., M, N and M_{des}, N_{des}) and the actual moments exerted by the propulsion system for the simulation of Figure 11 with the SVD-decoupling approach. The greatest error level is observable in the case of the pitching moment at the time of the yaw angle step movement, which is when the propulsion system cross-coupling is at its highest.

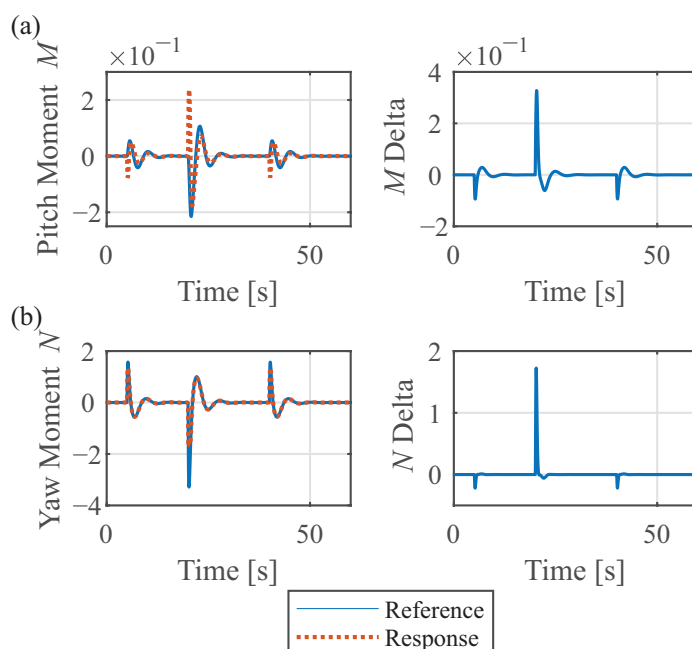


Figure 12. (a) Pitch moment M for varying yaw ψ input from decoupling control. (b) Yaw moment N for varying yaw ψ input from decoupling control.

3.1.3. Discussion

The previous results show that, in a simulated environment, the SVD-decoupling approach is effective in reducing the resulting cross-coupling, even when considering non-linear propulsion dynamics. In addition, the proper setting of the free variables when

calculating the propulsion system inverse dynamics allowed obtaining similar responses to the physical insight approach. That is, the SVD-decoupling approach allows integrating physical insight easily. This is an important feature, because in most real applications, practical considerations have to be taken into account. For example, Figure 13 presents a comparison between the tilt-rotor angles for the simulations of the previous section considering both control allocation approaches. This figure shows that both approaches essentially produce the same overall tilt-rotor angles; however, the SVD-decoupling approach introduces slight adjustments, which resulted in a reduced cross-coupling.

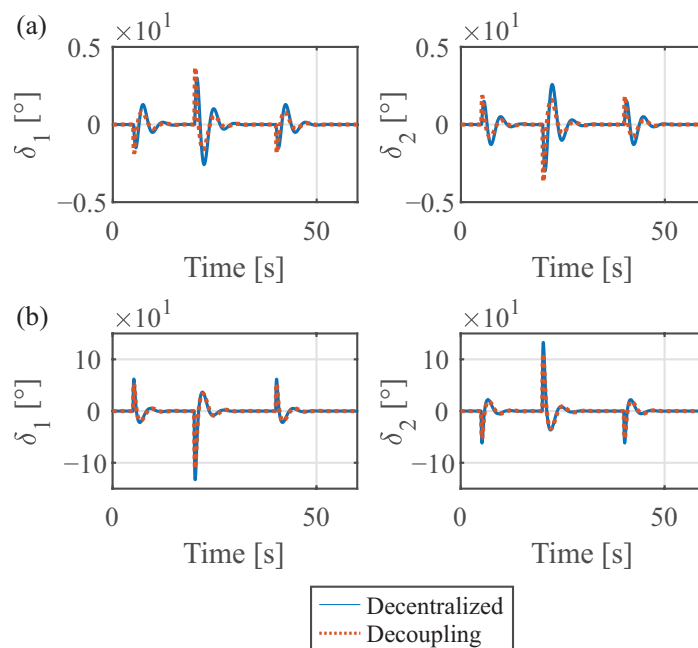


Figure 13. (a) Rotor angles δ_1, δ_2 from decentralized and decoupling controllers for a Pitch θ varying input. (b) Rotor angles δ_1, δ_2 from decentralized and decoupling controllers for a Yaw ψ varying input.

3.2. Experimental Results

The control system of Figure 8 was implemented experimentally using the test bench of Figure 3 and a similar set of experiments to those presented in the simulations was performed.

The PID gains of the previous section (i.e., simulation) were taken as a baseline in the tuning of the prototype’s controller. Since the simulated test bench equations (Equation (19)) did not account for friction damping, a slight adjustment of the PID gains was necessary to maintain the control specifications. A comparison of the frequency-domain response of the original (i.e., simulated) and the experimentally adjusted PID controllers is presented in Figure 14. This figure confirms that the main differences between these controllers are (1) decreased phase (damping) in the experiment and (2) increased gain for the experimental PID controller, which is in line with the effects of a higher level of friction in the experimental setup. The resulting PID gains used for the experiments are presented in Table 4. Both control allocation schemes were implemented using the same PID controllers.

Table 4. Experimental PID controller gains.

Constant	Pitch	Yaw
Proportional	1.5	1.5
Integral	1	0.5
Derivative	0.5	1

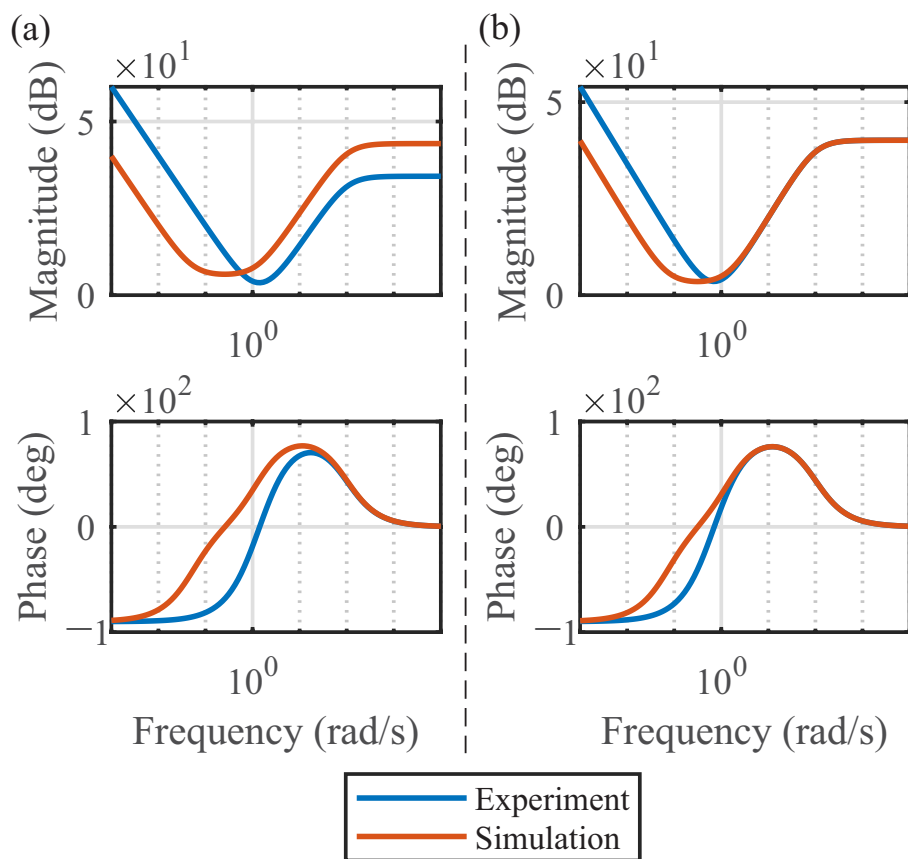


Figure 14. (a) Pitch θ moment PID controller bode diagrams for simulation and experiment. (b) Yaw ψ moment PID controller bode diagrams for simulation and experiment.

3.2.1. Pitch-Varying Case

The experimental responses of the test bench when the pitch reference is modified for both control allocation approaches are shown in Figure 15. In comparison with the simulated responses from Figure 9, this figure shows that the pitch angle responses are more affected by the amplitude of the pitch angle variation in both approaches. For instance, the overshoot when moving the pitch angle reference from 20° to -20° is larger than in the simulated response. This could be mostly due to actuator saturation (absolute or rate) or other non-modelled dynamics. The effect is that the cross-coupling reduction in the yaw angle of the SVD-decoupling approach is reduced in the largest pitch reference modification (40° magnitude), but it is maintained in the other cases (20° magnitude). In addition, a greater reduction was observed for the positive pitch angle variation than the corresponding negative of the same magnitude. This suggests that there could be imbalances in the test bench, either mechanical or due to actuator mismatch.

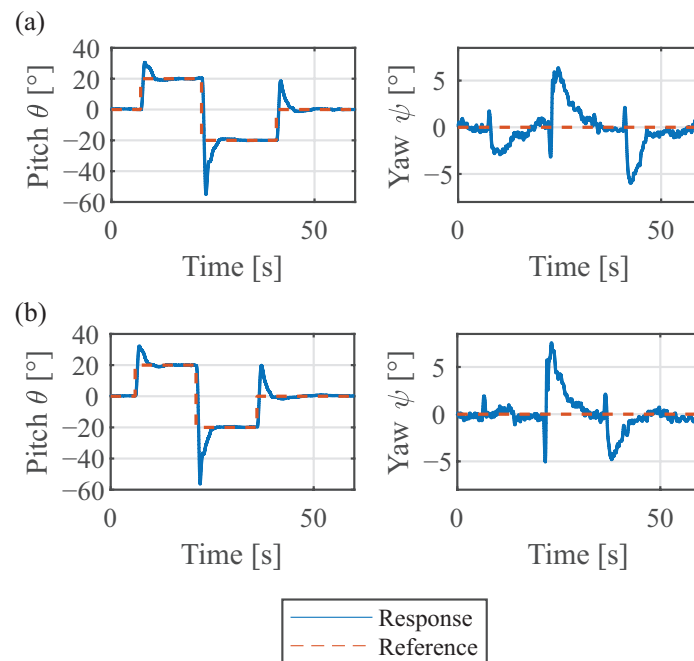


Figure 15. Pitch θ varying experimental responses. (a) Decentralized control allocation approach. (b) SVD-decoupling control allocation approach.

3.2.2. Yaw-Varying Case

Figure 16 shows the experimental results when varying the yaw angle reference. In this case, the cross-coupling reduction in the pitch angle introduced by the SVD-decoupling approach is maintained in all cases, while the overall yaw angle response performance is similar for both approaches. The contrast with the pitch-varying case, where the cross-coupling was greater in the largest magnitude reference change, suggests an asymmetry in the response times of the main pitch and yaw actuators (i.e., electronic speed controllers for pitch and tilt servos for yaw in this case).

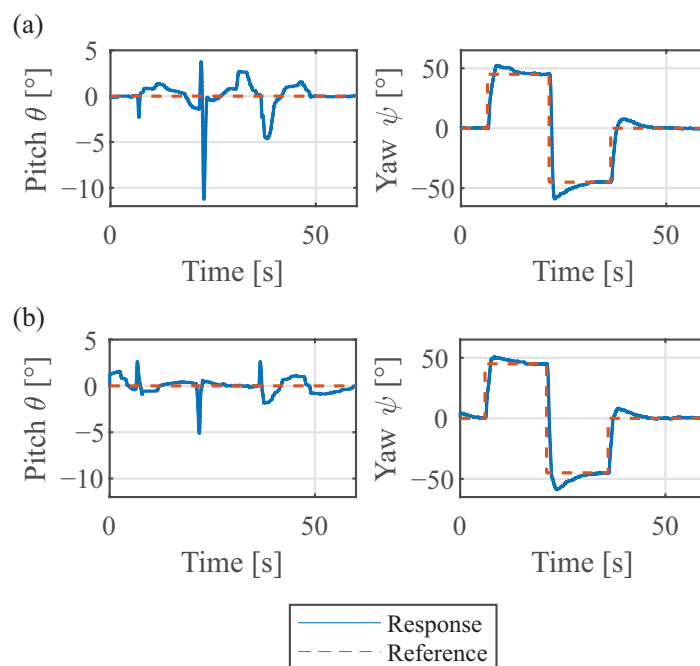


Figure 16. Yaw ψ varying experimental responses. (a) Decentralized control allocation approach. (b) SVD-decoupling control allocation approach.

3.3. Quantitative Analysis

A quantitative summary of the experimental responses is presented in Table 5, which shows the *Mean Squared Error (MSE)* of the experimental responses of Figures 15 and 16.

Comparing both control allocation approaches when varying the pitch angle reference, there was a reduction of 20.4% in the MSE of the yaw angle cross-coupling when using the SVD-decoupling scheme. A reduction of 70.5% in the MSE of the pitch angle cross-coupling was also observed when the yaw angle reference was modified with the SVD-decoupling scheme.

On the other hand, Table 5 also reveals that, interestingly, the cross-coupling reductions of the SVD-based scheme came at the cost of a slight increase in MSE at the reference angle responses. In particular, increases of 2.15% and 1.59% were observed for the pitch and yaw angles, respectively.

This trade-off of cross-coupling reduction and main angle tracking performance was not observed in the simulated responses, which suggests again that actuator limitations and asymmetry may be a possible explanation.

Figures 17 and 18 present the error distribution of the experimental responses. A closer look at Figure 17, which corresponds to the experiment where the pitch angle reference is modified, shows that the error distribution for the yaw angle is considerably reduced with the SVD-decoupling approach, with much tighter quartiles overall, while the median is similarly close to zero in both cases. In contrast, for the pitch angle, the SVD-decoupling approach yields similarly large quartiles with a slightly larger range. In addition, the distribution of the inner quartiles with the SVD-decoupling approach is significantly skewed compared with the decentralized approach, while maintaining the same overall size, resulting in the median being farther from zero in the SVD-decoupling approach, which can explain the slight increase of MSE in this case.

In the case of the yaw varying experiment, Figure 18 shows that the error distribution of the pitch angle, which represents the cross-coupling in this experiment, is also considerably reduced with the SVD-decoupling approach, with all quartiles much closer to zero as well as the median. For the yaw angle, the SVD-decoupling approach yields a very similar error distribution to the decentralized approach, with the main differences being a median closer to zero and a slight skew to negative errors for the outer quartiles.

These figures confirm and extend the observations made with Table 5. That is, introducing the SVD-decoupling scheme reduces the cross coupling significantly while only slightly affecting the reference angle performance.

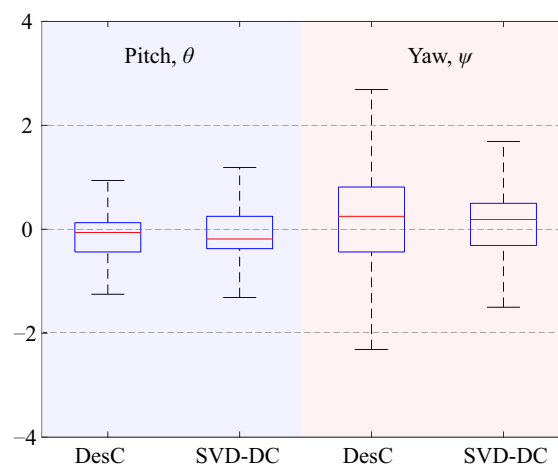


Figure 17. Error distribution of the experimental responses of the pitch θ varying experiment. DesC = decentralized control. SVD-DC = SVD decoupling control.

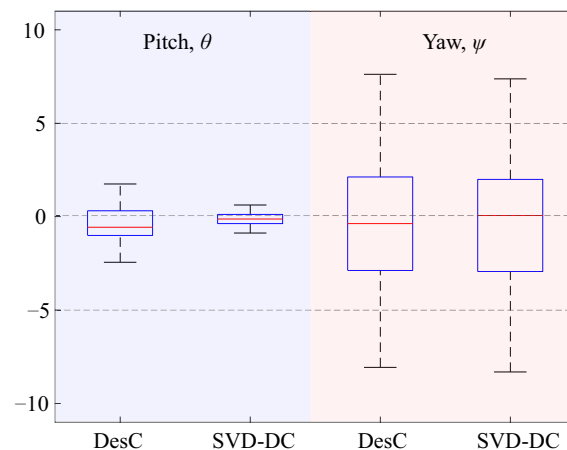


Figure 18. Error distribution of the experimental responses of the yaw ψ varying experiment. DesC = decentralized control. SVD-DC = SVD decoupling control.

Table 5. Mean Squared Error comparison between decentralized and decoupling controllers for pitch θ and yaw ψ reference variations.

Experiment	DoF	Decentralized	Decoupling	$\Delta\%$
Pitch θ Variation	Pitch θ	37.4525	38.2600	2.1560
	Yaw ψ	4.1196	3.2768	−20.4583
Yaw ψ Variation	Pitch θ	2.3904	0.7042	−70.5405
	Yaw ψ	118.6156	120.5088	1.5960

4. Discussion and Conclusions

In this article, a modified PVTOL configuration with an arbitrary number of co-linear tilting rotors was introduced as a baseline to study the control allocation problem found in many of the recently proposed VTOL aircraft designs. A general model for the resulting propulsion subsystem, as well as its linearization, was also developed. This linearization, which is necessary for many of the current control allocation strategies, is presented in a general and structured manner, to facilitate a better understanding of the effects of each of the physical parameters of the propulsion system.

Following the proposed modified PVTOL configuration, a two-tilting-rotor test bench was implemented experimentally. This test bench yields an over-actuated system which can be used to study the control allocation problem theoretically and experimentally. An SVD control allocation approach was developed for the resulting test bench. The proposed approach allows deriving an adequate input mixer algorithm for the over-actuated system, and it is shown that the remaining free degrees of freedom can be used to integrate physical insight and to solve general optimization goals (in this case, the minimization of error due to linearization).

The resulting SVD control allocation scheme is compared with a more traditional scheme derived by physical insight. It is shown that both approaches yield a similar use of the available control variables, with the SVD-based scheme introducing minor input modifications which allow obtaining a considerable decrease in cross-coupling in the test bench orientation angles.

Simulation and experimental results validate that the SVD control allocation scheme allows decreasing cross-coupling while maintaining the same overall performance as the traditional approach. The main deviations from the simulated and experimental results are due to the presence of friction damping in the experimental test bench, which was expected.

Interestingly, other smaller deviations suggest that actuator discrepancies can also have a significant effect on the resulting performance, that is, differences in actuator time responses, saturation levels, etc., due to the type of actuator, for instance, tilt-rotor

servo dynamics vs. electric motor controller and propeller dynamics. Further research which incorporates better specific actuator properties is required to extend the benefits of decoupling control allocation schemes in general. This is an important finding, since many applications which require control allocation solutions use a mixture of dissimilar actuators.

Finally, the results support the continued use of the proposed modified PVTOL configuration, in either the presented two-rotor version or in a more complex configuration, for the study of the control allocation problem.

Author Contributions: Conceptualization, L.A.-B. and D.H.-A.; methodology, L.A.-B.; software, E.M.-M.; validation, L.A.-B., D.H.-A. and E.M.-M.; formal analysis, L.A.-B. and E.M.-M.; investigation, L.A.-B. and E.M.-M.; resources, L.A.-B. and D.H.-A.; data curation, E.M.-M.; writing—original draft preparation, L.A.-B. and E.M.-M.; writing—review and editing, D.H.-A.; visualization, E.M.-M.; supervision, L.A.-B. and D.H.-A.; project administration, L.A.-B. and D.H.-A.; funding acquisition, L.A.-B. and D.H.-A. All authors have read and agreed to the published version of the manuscript.

Funding: This research received no external funding.

Data Availability Statement: Data are contained within the article.

Conflicts of Interest: The authors declare no conflict of interest.

References

1. EASA. MOC SC-VTOL, *Proposed Means of Compliance with the Special Condition VTOL*; Technical Report; European Union Aviation Safety Agency: Cologne, Germany, 2022.
2. EASA. RMT.0731, *Terms of Reference for Rulemaking Task, New Air Mobility*; Technical Report; European Union Aviation Safety Agency: Cologne, Germany, 2021.
3. Wang, X.; Cai, L. Mathematical modeling and control of a tilt-rotor aircraft. *Aerosp. Sci. Technol.* **2015**, *47*, 473–492. [[CrossRef](#)]
4. Kong, Z.; Lu, Q. Mathematical Modeling and modal switching control of a novel tiltrotor UAV. *J. Robot.* **2018**, *2018*, 8641731. [[CrossRef](#)]
5. Lu, K.; Liu, C.; Li, C.; Chen, R. Flight Dynamics Modeling and Dynamic Stability Analysis of tilt-rotor aircraft. *Int. J. Aerosp. Eng.* **2019**, *2019*, 5737212. [[CrossRef](#)]
6. Sheng, H.; Zhang, C.; Xiang, Y. Mathematical Modeling and Stability Analysis of tiltrotor aircraft. *Drones* **2022**, *6*, 92. [[CrossRef](#)]
7. Çakıcı, F.; Leblebicioğlu, M.K. Modeling and simulation of a small-sized tiltrotor UAV. *J. Def. Model. Simul. Appl. Methodol. Technol.* **2011**, *9*, 335–345. [[CrossRef](#)]
8. Chen, C.; Shen, L.; Zhang, D.; Zhang, J. Mathematical Modeling and control of a tiltrotor UAV. In Proceedings of the 2016 IEEE International Conference on Information and Automation (ICIA), Ningbo, China, 1–3 August 2016. [[CrossRef](#)]
9. Liu, Z.; He, Y.; Yang, L.; Han, J. Control techniques of Tilt Rotor Unmanned Aerial Vehicle Systems: A Review. *Chin. J. Aeronaut.* **2017**, *30*, 135–148. [[CrossRef](#)]
10. Hegde, N.T.; George, V.; Nayak, C.G.; Kumar, K. Design, dynamic modelling and control of tilt-rotor uavs: A Review. *Int. J. Intell. Unmanned Syst.* **2019**, *8*, 143–161. [[CrossRef](#)]
11. Bacchini, A.; Cestino, E. Electric VTOL Configurations Comparison. *Aerospace* **2019**, *6*, 26. [[CrossRef](#)]
12. Amezcua-Brooks, L.; Liceaga-Castro, E.; Gonzalez-Sanchez, M.; Garcia-Salazar, O.; Martinez-Vazquez, D. Towards a standard design model for quad-rotors: A review of current models, their accuracy and a novel simplified model. *Prog. Aerosp. Sci.* **2017**, *95*, 1–23. [[CrossRef](#)]
13. Amezcua-Brooks, L.; Hernandez-Alcantara, D.; Santana-Delgado, C.; Covarrubias-Fabela, R.; Garcia-Salazar, O.; Ramirez-Mendoza, A.M.E. Improved Model for Micro-UAV Propulsion Systems: Characterization and Applications. *IEEE Trans. Aerosp. Electron. Syst.* **2020**, *56*, 2174–2197. [[CrossRef](#)]
14. Grau, S.; Kapitola, S.; Weiss, S.; Noack, D. Control of an over-actuated spacecraft using a combination of a fluid actuator and reaction wheels. *Acta Astronaut.* **2021**, *178*, 870–880. [[CrossRef](#)]
15. Qin, Z.; Liu, K.; Zhao, X. A smooth control allocation method for a distributed electric propulsion VTOL aircraft test platform. *IET Control Theory Appl.* **2023**, *17*, 925–942. [[CrossRef](#)]
16. Santos, M.; Honório, L.; Moreira, A.; Garcia, P.; Silva, M.; Vidal, V. Analysis of a Fast Control Allocation approach for nonlinear over-actuated systems. *ISA Trans.* **2022**, *126*, 545–561. [[CrossRef](#)] [[PubMed](#)]
17. Hamandi, M.; Usai, F.; Sablé, Q.; Staub, N.; Tognon, M.; Franchi, A. Design of multirotor aerial vehicles: A taxonomy based on input allocation. *Int. J. Robot. Res.* **2021**, *40*, 027836492110259. [[CrossRef](#)]
18. Zheng, X.; Yang, X. Improved adaptive NN backstepping control design for a perturbed PVTOL aircraft. *Neurocomputing* **2020**, *410*, 51–60. [[CrossRef](#)]
19. Bonilla, M.; Blas, L.; Azhmyakov, V.; Malabre, M.; Salazar, S. Robust structural feedback linearization based on the nonlinearities rejection. *J. Frankl. Inst.* **2020**, *357*, 2232–2262. [[CrossRef](#)]

20. Łakomy, K.; Madonski, R. Cascade extended state observer for active disturbance rejection control applications under measurement noise. *ISA Trans.* **2021**, *109*, 1–10. [[CrossRef](#)] [[PubMed](#)]
21. Offermann, A.; Castillo, P.; Miras, J.D. Control of a PVTOL with tilting rotors. In Proceedings of the 2019 International Conference on Unmanned Aircraft Systems (ICUAS), Atlanta, GA, USA, 11–14 June 2019. [[CrossRef](#)]
22. Harindranath, A.; Arora, M. A Systematic Review of User-Conducted Calibration Methods for MEMS-based IMUs. *Measurement* **2023**, 114001. [[CrossRef](#)]
23. Otegui, J.; Bahillo, A.; Lopetegi, I.; Díez, L.E. Performance Evaluation of Different Grade IMUs for Diagnosis Applications in Land Vehicular Multi-Sensor Architectures. *IEEE Sens. J.* **2021**, *21*, 2658–2668. [[CrossRef](#)]
24. de Alteriis, G.; Conte, C.; Lo Moriello, R.S.; Accardo, D. Use of Consumer-Grade MEMS Inertial Sensors for Accurate Attitude Determination of Drones. In Proceedings of the 2020 IEEE 7th International Workshop on Metrology for AeroSpace (MetroAeroSpace), Pisa, Italy, 22–24 June 2020; pp. 534–538. [[CrossRef](#)]
25. Villarreal Valderrama, J.F.; Takano, L.; Liceaga-Castro, E.; Hernandez-Alcantara, D.; Zambrano-Robledo, P.D.C.; Amezcua-Brooks, L. An integral approach for aircraft pitch control and instrumentation in a wind-tunnel. *Aircr. Eng. Aerosp. Technol.* **2020**, *92*, 1111–1123. [[CrossRef](#)]

Disclaimer/Publisher’s Note: The statements, opinions and data contained in all publications are solely those of the individual author(s) and contributor(s) and not of MDPI and/or the editor(s). MDPI and/or the editor(s) disclaim responsibility for any injury to people or property resulting from any ideas, methods, instructions or products referred to in the content.